

The asymptotics of a generalised Beta function

R. B. Paris

Division of Computing and Mathematics,
University of Abertay Dundee, Dundee DD1 1HG, UK

Abstract

We consider the generalised Beta function introduced by Chaudhry *et al.* [J. Comp. Appl. Math. **78** (1997) 19–32] defined by

$$B(x, y; p) = \int_0^1 t^{x-1} (1-t)^{y-1} \exp\left[\frac{-p}{4t(1-t)}\right] dt,$$

where $\Re(p) > 0$ and the parameters x and y are arbitrary complex numbers. The asymptotic behaviour of $B(x, y; p)$ is obtained when (i) p large, with x and y fixed, (ii) x and p large, (iii) x , y and p large and (iv) either x or y large, with p finite. Numerical results are given to illustrate the accuracy of the formulas obtained.

Mathematics Subject Classification: 30E15, 33B15, 34E05, 41A60

Keywords: Generalised Beta function, asymptotic expansion, Mellin-Barnes integral, method of steepest descents

1. Introduction

In [1], Chaudhry *et al.* introduced a generalised beta function defined by the Euler-type integral¹

$$B(x, y; p) = \int_0^1 t^{x-1} (1-t)^{y-1} \exp\left[\frac{-p}{4t(1-t)}\right] dt, \quad (1.1)$$

where $\Re(p) > 0$ and the parameters x and y are arbitrary complex numbers. When $p = 0$, it is clear that when $\Re(x) > 0$ and $\Re(y) > 0$ the generalised function reduces to the well-known beta function $B(x, y)$ of classical analysis. The justification for defining this extension of the beta function is given in [1] and an application of its use in defining extensions of the Gauss and confluent hypergeometric functions is discussed in [2]. It is evident from the definition in (1.1) that $B(x, y; p)$ satisfies the symmetry property

$$B(x, y; p) = B(y, x; p). \quad (1.2)$$

A list of useful properties of $B(x, y; p)$ is detailed by Miller in [4], where it is established that $B(x, y; p)$ may be expanded as an infinite series of Whittaker functions or Laguerre polynomials; see (A.1). He also obtained a Mellin-Barnes integral representation for

¹The factor 4 is introduced in the exponential for presentational convenience.

$B(x, y; p)$, which we exploit in Section 2, and expressed $B(x, x \pm n; p)$ and $B(1 \pm n, 1; p)$, where n is an integer, as finite sums of Whittaker functions.

Our aim in this note is to derive asymptotic expansions for $B(x, y; p)$ for large x, y and p . We consider (i) $|p| \rightarrow \infty$ in $|\arg p| < \frac{1}{2}\pi$, with x and y fixed, (ii) x and p large, (iii) x, y and p large and (iv) either x or y large, with p finite. The expansion for large p is obtained using a Mellin-Barnes integral representation for $B(x, y; p)$, whereas the other cases are obtained using the method of steepest descents.

2. The expansion of $B(x, y; p)$ for large p with x, y finite

We start with the Mellin-Barnes integral representation given by Miller [4]

$$B(x, y; p) = 2^{1-x-y} \pi^{\frac{1}{2}} \frac{1}{2\pi i} \int_{c-\infty i}^{c+\infty i} \frac{\Gamma(s)\Gamma(x+s)\Gamma(y+s)}{\Gamma(\frac{1}{2}x+\frac{1}{2}y+s)\Gamma(\frac{1}{2}x+\frac{1}{2}y+\frac{1}{2}+s)} p^{-s} ds \tag{2.1}$$

valid in $|\arg p| < \frac{1}{2}\pi$, where $c > \max\{0, -\Re(x), -\Re(y)\}$ so that the integration path lies to the right of all the poles of the integrand situated at $s = -k, s = -x - k$ and $s = -y - k, k = 0, 1, 2, \dots$. Displacement of the integration path to the left over the poles followed by evaluation of the residues (assuming that no two members of the set $\{0, x, y\}$ differ by an integer – thereby avoiding the presence of higher-order poles) yields the result that $B(x, y; p)$ can be expressed as the sum of three ${}_2F_2(-\frac{1}{4}p)$ hypergeometric functions; see [4, Eq. (1.6)].

Since there are no poles in the half-plane $\Re(s) > c$ it follows that displacement of the integration path to the right can produce no algebraic-type asymptotic expansion; see [8, §5.4]. We can therefore displace the path as far to the right as we please; on such a displaced path, which we denote by L , the variable $|s|$ is everywhere large. The ratio of gamma functions in the integrand in (2.1) may then be expanded as an inverse factorial expansion given by [8, p. 39, Lemma 2.2]

$$\frac{\Gamma(s)\Gamma(x+s)\Gamma(y+s)}{\Gamma(\frac{1}{2}x+\frac{1}{2}y+s)\Gamma(\frac{1}{2}x+\frac{1}{2}y+\frac{1}{2}+s)} = \sum_{j=0}^{M-1} (-)^j c_j \Gamma(s-j-\frac{1}{2}) + \rho_M(s)\Gamma(s-M-\frac{1}{2}),$$

where M is a positive integer and $\rho_M(s) = O(1)$ as $|s| \rightarrow \infty$ in $|\arg s| < \pi$. The coefficients $c_j \equiv c_j(x, y)$ are discussed below where the leading coefficient $c_0 = 1$.

Substitution of the above inverse factorial expansion into the integral (2.1) then produces

$$B(x, y; p) = 2^{1-x-y} \pi^{\frac{1}{2}} \left\{ \sum_{j=0}^{M-1} (-)^j c_j \frac{1}{2\pi i} \int_L \Gamma(s-j-\frac{1}{2}) p^{-s} ds + R_M \right\},$$

where

$$R_M = \frac{1}{2\pi i} \int_L \rho_M(s)\Gamma(s-M-\frac{1}{2}) p^{-s} ds.$$

The integral may be evaluated by the well-known Cahen-Mellin integral given by (see, for example, [8, p. 90])

$$\frac{1}{2\pi i} \int_{c-\infty i}^{c+\infty i} \Gamma(s+\alpha) z^{-s} ds = z^\alpha e^{-z} \quad (|\arg z| < \frac{1}{2}\pi, c > -\Re(\alpha))$$

to yield

$$B(x, y; p) = 2^{1-x-y} \pi^{\frac{1}{2}} \left\{ p^{-\frac{1}{2}} e^{-p} \sum_{j=0}^{M-1} (-)^j c_j p^{-j} + R_M \right\}.$$

A bound for the remainder R_M has been considered in [8, p. 71, Lemma 2.7], from which it follows that $R_M = O(p^{-M-\frac{1}{2}} e^{-p})$ as $|p| \rightarrow \infty$ in $|\arg p| < \frac{1}{2}\pi$.

Hence we obtain the asymptotic expansion

$$B(x, y; p) = 2^{1-x-y} \pi^{\frac{1}{2}} p^{-\frac{1}{2}} e^{-p} \left\{ \sum_{j=0}^{M-1} (-)^j c_j p^{-j} + O(p^{-M}) \right\} \tag{2.2}$$

valid as $|p| \rightarrow \infty$ in the sector $|\arg p| < \frac{1}{2}\pi$. The expansion of $B(x, y; p)$ for large p is seen to be exponentially small in $|\arg p| < \frac{1}{2}\pi$; this is a standard result when there are no poles on the right of the path in (2.1) and routine path displacement does not produce any useful asymptotic information [8, §5.4].

The coefficients c_j for $j \geq 1$ can be generated by the algorithm described in [8, §2.2.4]. It is found that

$$c_1 = \frac{1}{4}(1 + x + y + 2xy - x^2 - y^2),$$

$$c_2 = \frac{1}{32}(9 + 6(2 + xy)(x + y + xy) - (7 + 4xy)(x^2 + y^2) - 6(x^3 + y^3) + x^4 + y^4 + 14xy),$$

which are symmetrical in x and y as required by (1.2). A closed-form representation for c_j is derived in the appendix, where it is shown that c_j can be expressed in terms of a terminating ${}_3F_2(1)$ hypergeometric function given by

$$c_j \equiv c_j(x, y) = \frac{(\frac{1}{2})_j (y + \frac{1}{2})_j}{j!} {}_3F_2 \left[\begin{matrix} -j, \frac{1}{2}y - \frac{1}{2}x, \frac{1}{2}y - \frac{1}{2}x + \frac{1}{2} \\ \frac{1}{2}, y + \frac{1}{2} \end{matrix}; 1 \right], \tag{2.3}$$

where $(a)_j = \Gamma(a + j)/\Gamma(a)$ is the Pochhammer symbol. When $x = y$, this reduces to the simpler expression

$$c_j(x, x) = \frac{(\frac{1}{2})_j (x + \frac{1}{2})_j}{j!}. \tag{2.4}$$

We remark that the asymptotic expansion of $B(x, y; p)$ for $p \rightarrow \infty$ could also have been obtained by application of the method of steepest descents, which we shall employ in the subsequent sections. See also the appendix for a different approach.

3. The expansion of $B(x, y; p)$ for large x and p with y finite

We consider the expansion of $B(x, y; p)$ for large x and p , with y finite, when it is supposed that $p = ax$, where $a > 0$ and $|\arg x| < \frac{1}{2}\pi$. By the symmetry property (1.2), the same result will also cover the case of large y and p , with x finite. From (1.1), we have

$$B(x, y; ax) = \int_0^1 f(t) e^{-x\psi(t)} dt \quad (|\arg x| < \frac{1}{2}\pi), \tag{3.1}$$

where

$$\psi(t) = \frac{a}{4t(1-t)} - \log t, \quad f(t) = \frac{(1-t)^y}{t}.$$

Saddle points of the exponential factor are given by $\psi'(t) = 0$; that is, at the roots of the cubic

$$t(1-t)^2 + \frac{1}{4}a(1-2t) = 0. \tag{3.2}$$

We label the three saddles t_0 , t_1 and t_2 . All three saddles lie on the real axis with t_0 situated in the closed interval $[0, 1]$, with $t_1 > 1$ and $t_2 < 0$. The t -plane is cut along $(-\infty, 0]$. Paths of steepest descent through the saddles t_r ($r = 0, 1$) are given by

$$\Im\{e^{i\theta}(\psi(t) - \psi(t_r))\} = 0, \quad \theta = \arg x;$$

these paths terminate at $t = 0$ and $t = 1$ in the directions $|\theta - \phi| < \frac{1}{2}\pi$ and $\frac{1}{2}\pi < \theta - \phi < \frac{3}{2}\pi$, respectively, where $\phi = \arg t$.

When $x > 0$, the integration path coincides with the steepest descent path over the saddle t_0 ; for complex x in the sector $|\arg x| < \frac{1}{2}\pi$, the steepest descent path through t_0 becomes deformed but still terminates at $t = 0$ and $t = 1$; see Fig. 1. Application of the

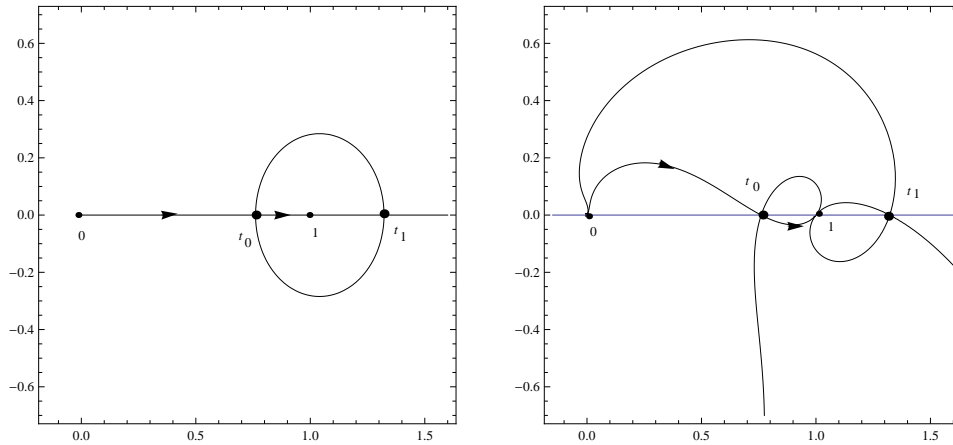


Figure 1: The steepest descent and ascent paths through the saddles t_0 and t_1 (heavy dots) when $a = 1/3$ and (a) $\theta = 0$ and (b) $\theta = \pi/4$. The arrows indicate the integration path. In (b) the steepest ascent paths spiral round $t = 0$ out to infinity passing onto adjacent Riemann surfaces. The saddle t_2 on the branch cut on $(-\infty, 0]$ is not shown.

saddle-point method then yields the leading behaviour

$$\begin{aligned} B(x, y; ax) &\sim \sqrt{\frac{2\pi}{x\psi''(t_0)}} f(t_0)e^{-x\psi(t_0)} \\ &= \sqrt{\frac{2\pi}{x\psi''(t_0)}} t_0^{x-1}(1-t_0)^{y-1} \exp\left[\frac{-ax}{4t_0(1-t_0)}\right] \end{aligned} \quad (3.3)$$

as $|x| \rightarrow \infty$ in the sector $|\arg x| < \frac{1}{2}\pi$, where some routine algebra combined with (3.2) shows that

$$\psi''(t_0) = \frac{1 - 3t_0 + 4t_0^2}{t_0^2(1-t_0)(2t_0-1)}.$$

We remark that the saddle $t_0 \equiv t_0(a)$ has to be computed for a particular value of the parameter a , either directly from (3.2) or as a cubic root.

The asymptotic expansion of $B(x, y; ax)$ is given by [7, p. 47]

$$B(x, y; ax) \sim 2e^{-x\psi(t_0)} \sum_{n=0}^{\infty} \frac{C_{2n}\Gamma(n + \frac{1}{2})}{x^{n+\frac{1}{2}}} \quad (|x| \rightarrow \infty, |\arg x| < \frac{1}{2}\pi). \quad (3.4)$$

The coefficients C_n can be obtained by an inversion process and are listed for $n \leq 8$ in [3, p. 119] and for $n \leq 4$ in [9, p. 13]. Alternatively, they can be obtained by an expansion process to yield Wojdylo's formula [10] given by

$$C_n = \frac{1}{2a_0^{(n+1)/2}} \sum_{k=0}^n b_{n-k} \sum_{j=0}^k \frac{(-)^j (\frac{1}{2}n + \frac{1}{2})_j}{j! a_0^j} B_{kj}; \quad (3.5)$$

see also [5, 6]. Here $B_{kj} \equiv B_{kj}(a_1, a_2, \dots, a_{k-j+1})$ are the partial ordinary Bell polynomials generated by the recursion²

$$B_{kj} = \sum_{r=1}^{k-j+1} a_r B_{k-r, j-1}, \quad B_{k0} = \delta_{k0},$$

where δ_{mn} is the Kronecker symbol, and the coefficients a_r and b_r appear in the expansions

$$\psi(t) - \psi(t_0) = \sum_{r=0}^{\infty} a_r (t - t_0)^{r+2}, \quad f(t) = \sum_{r=0}^{\infty} b_r (t - t_0)^r \quad (3.6)$$

valid in a neighbourhood of the saddle $t = t_0$.

In numerical computations we choose a value of the parameter a and compute the saddle t_0 from (3.2). With a value of y , *Mathematica* is used to determine the coefficients a_r and b_r for $0 \leq r \leq n_0$. The coefficients C_{2n} can then be calculated for $0 \leq n \leq n_0$ from (3.5). We display the computed values of C_{2n} for different values of a and y in Table 1. In Table 2, the values of the absolute relative error in the computation of $B(x, y; ax)$ from (3.4) are presented as a function of the truncation index n when $x = 100$.

Table 1: Values of the coefficients C_{2n} (to 10dp) for different a and y .

n	$a = 1, y = 1$	$a = \frac{1}{2}, y = \frac{3}{2}$	$a = \frac{3}{2}, y = \frac{5}{4}$	$a = 2, y = \frac{1}{2}$
0	+0.2668661228	+0.1364219142	+0.2036093538	+0.3909054941
1	+0.0982652355	+0.2683838462	+0.0762869817	-0.0309094064
2	-0.0635656655	-0.1085963949	-0.0456489054	-0.0039290992
3	+0.0186002666	+0.0151339630	+0.0137423943	+0.0024209801
4	-0.0039253710	-0.0003383888	-0.0026770977	-0.0005115807
5	+0.0012059654	+0.0004533741	+0.0003423270	+0.0000299402

4. The expansion of $B(x, y; p)$ for large x, y and p

We consider the expansion of $B(x, y; p)$ for large x, y and p , when it is supposed that $p = ax$ and $y = bx$, where $a > 0, b > 0$ and $|\arg x| < \frac{1}{2}\pi$. From (1.1), we have

$$B(x, y; p) = \int_0^1 f(t) e^{-x\psi(t)} dt \quad (|\arg x| < \frac{1}{2}\pi), \quad (4.1)$$

²For example, this generates the values $B_{41} = a_4, B_{42} = a_3^2 + 2a_1a_3, B_{43} = 3a_1^2a_2$ and $B_{44} = a_1^4$.

Table 2: Values of the absolute relative error in $B(x, y; ax)$ when $x = 100$ for different truncation index.

n	$a = 1, y = 1$	$a = \frac{1}{2}, y = \frac{3}{2}$	$a = \frac{3}{2}, y = \frac{5}{4}$	$a = 2, y = \frac{1}{2}$
0	1.838×10^{-3}	9.682×10^{-3}	1.853×10^{-3}	3.963×10^{-4}
1	1.770×10^{-5}	5.892×10^{-5}	1.666×10^{-5}	7.426×10^{-7}
2	1.295×10^{-7}	2.058×10^{-7}	1.255×10^{-7}	1.153×10^{-8}
3	9.506×10^{-10}	1.517×10^{-10}	8.562×10^{-10}	8.568×10^{-11}
4	1.295×10^{-11}	9.526×10^{-12}	5.011×10^{-12}	2.332×10^{-13}
5	3.688×10^{-12}	1.933×10^{-13}	5.472×10^{-14}	6.917×10^{-15}

where

$$\psi(t) = \frac{a}{4t(1-t)} - \log t - b \log(1-t), \quad f(t) = \frac{1}{t(1-t)}. \tag{4.2}$$

Saddle points of the exponential factor are given by the roots of the cubic

$$t(1-t)\{1 - (b+1)t\} + \frac{1}{4}a(1-2t) = 0. \tag{4.3}$$

Routine examination of this cubic shows that, when $a > 0, b > 0$, all roots are real, with one root greater than 1, one in the interval $[0, 1]$ and one negative root. The distribution of the saddles is thus similar to that in Section 3, where we continue to label the saddle situated in $[0, 1]$ by t_0 . The topology of the path of steepest descent through the saddle t_0 , given by $\Im\{e^{i\theta}(\psi(t) - \psi(t_0))\} = 0$ where $\theta = \arg x$, is also similar to that depicted in Fig. 1.

Accordingly, the expansion of $B(x, y; p)$ when $p = ax$ and $y = bx$, with $a > 0, b > 0$, is given by

$$B(x, bx; ax) \sim 2e^{-x\psi(t_0)} \sum_{n=0}^{\infty} \frac{C_{2n}\Gamma(n + \frac{1}{2})}{x^{n+\frac{1}{2}}} \quad (|x| \rightarrow \infty, |\arg x| < \frac{1}{2}\pi), \tag{4.4}$$

where the coefficients C_{2n} can be determined from (3.5) when the coefficients a_r and b_r in (3.6) are evaluated from the definitions of $\psi(t)$ and $f(t)$ in (4.2).

The leading behaviour is

$$\begin{aligned} B(x, bx; ax) &\sim \sqrt{\frac{2\pi}{x\psi''(t_0)}} f(t_0)e^{-x\psi(t_0)} \\ &= \sqrt{\frac{2\pi}{x\psi''(t_0)}} t_0^{x-1}(1-t_0)^{bx-1} \exp\left[\frac{-ax}{4t_0(1-t_0)}\right] \end{aligned} \tag{4.5}$$

as $|x| \rightarrow \infty$ in the sector $|\arg x| < \frac{1}{2}\pi$, where

$$\psi''(t_0) = \frac{1 - 3t_0 + 4t_0^2}{t_0^2(1-t_0)(2t_0-1)} \left(1 - \frac{bt_0}{1-t_0}\right) + \frac{b}{t_0(1-t_0)^2}$$

and $t_0 \equiv t_0(a, b)$ is the root of (4.3) situated in $t \in [0, 1]$.

We note that when $b = 1$ we have the result [1, 4]

$$B(x, x; p) = 2^{1-2x} \pi^{\frac{1}{2}} p^{(x-1)/2} e^{-\frac{1}{2}p} W_{-\frac{1}{2}x, \frac{1}{2}x}(p)$$

in terms of the Whittaker function $W_{\kappa, \mu}(z)$; see (A.1).

5. The behaviour of $B(x, y; p)$ for large x and finite y and p

In this final section, we examine the behaviour of $B(x, y; p)$ for large complex $x = |x|e^{i\theta}$, with $0 \leq \theta \leq \pi$, when y and $p > 0$ are finite. The situation when $-\pi \leq \theta \leq 0$ is analogous and, in the case of real y , $B(x, y; p)$ assumes conjugate values. This case has been discussed in [2, Appendix], but is repeated (with minor corrections) here for completeness. By the symmetry property (1.2), the same result will also cover the case of large y , with x and p finite.

From (1.1), we have upon interchanging x and y (by virtue of (1.2))

$$B(x, y; p) = \int_0^1 f(t)e^{-|x|\psi(t)} dt, \tag{5.1}$$

where

$$\psi(t) = \frac{\alpha}{t(1-t)} - e^{i\theta} \log(1-t), \quad f(t) = \frac{t^{y-1}}{1-t}, \quad \alpha := \frac{p}{4|x|}. \tag{5.2}$$

Because $p > 0$ is a fixed parameter, the integral (5.1) is valid for arbitrary complex values of x and y . Saddle points of the exponential factor arise when $\psi'(t) = 0$; that is, when

$$t^2(t-1) + \alpha e^{-i\theta}(1-2t) = 0. \tag{5.3}$$

We label the three saddles t_0, t_1 and t_2 as in Section 3. When $\theta = 0$, all three saddles are situated on the real axis with $t_0 \in [0, 1]$ and $t_1 > 1, t_2 < 1$. As θ increases, the saddles t_0 and t_2 rotate about the origin and t_1 rotates about the point $t = 1$. The result of this rotation is that, when $\theta = \pi$, t_0 and t_2 become a complex conjugate pair near the origin and t_1 is situated in the interval $[0, 1]$; see Fig. 2.

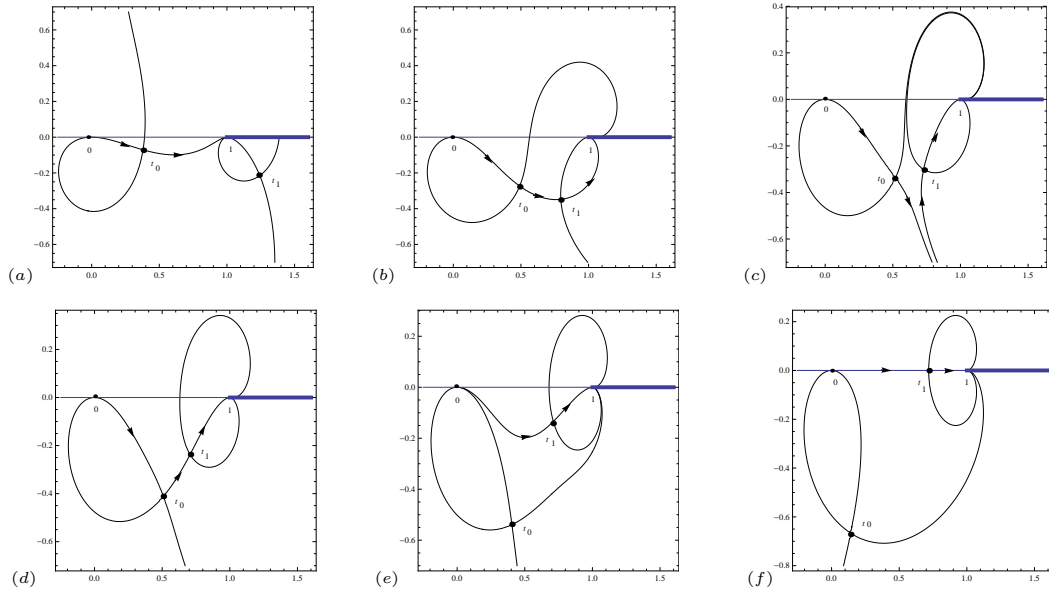


Figure 2: The steepest descent and ascent paths through the saddles t_0 and t_1 (heavy dots) when $\alpha = 1/3$ and (a) $\theta = 0.25\pi$, (b) $\theta = \theta_0 = 0.65595\pi$, (c) $\theta = 0.69\pi$, (d) $\theta = \theta_1 = 0.71782\pi$, (e) $\theta = 0.80\pi$ and (f) $\theta = \pi$. The arrows indicate the integration path. The steepest ascent paths spiral round $t = 1$ out to infinity passing onto adjacent Riemann surfaces. The saddle t_2 is not shown. The t -plane is cut along $[1, \infty)$.

When $\theta = 0$, the integration path coincides with the steepest descent path passing over the saddle t_0 given approximately by

$$t_0 \simeq \alpha^{\frac{1}{2}} - \frac{1}{2}\alpha \quad (x \rightarrow \infty).$$

Then, with the estimates

$$x\psi(t_0) \simeq (px)^{1/2} + \frac{3}{8}p, \quad \psi''(t_0) \simeq 2\alpha^{-\frac{1}{2}},$$

we find by application of the saddle-point method the leading behaviour

$$B(x, y; p) \sim \sqrt{\frac{\pi}{x}} \left(\frac{p}{4x}\right)^{\frac{1}{2}y - \frac{1}{4}} \exp\left[-(px)^{1/2} - \frac{3}{8}p\right] \quad (\theta = 0, x \rightarrow +\infty). \quad (5.4)$$

When $\theta = \pi$, we find from (5.3) that the saddle t_1 close to the point $t = 1$ is given by

$$t_1 \simeq 1 - \alpha + \alpha^3 \quad (|x| \rightarrow \infty)$$

and

$$|x|\psi(t_1) \simeq |x| + \frac{1}{4}p - |x|\log \alpha, \quad \psi''(t_1) \simeq \alpha^{-2}.$$

The integration path again coincides with the steepest descent path through t_1 , and so we obtain the behaviour

$$\begin{aligned} B(x, y; p) &\sim i\sqrt{\frac{2\pi}{x}} \left(\frac{p}{4x}\right)^x e^{\pi ix} \exp\left[x - \frac{1}{4}p\right] \quad (\theta = \pi, x \rightarrow -\infty) \\ &= \sqrt{\frac{2\pi}{|x|}} \left(\frac{p}{4|x|}\right)^{-|x|} \exp\left[-|x| - \frac{1}{4}p\right]. \end{aligned} \quad (5.5)$$

The leading terms in (5.4) and (5.5) were given in [2, Appendix].

A detailed study of the topology of the steepest descent paths³ through the saddles t_0 and t_1 when $0 \leq \theta \leq \pi$ is summarised in Fig. 2 for the particular case $\alpha = \frac{1}{3}$. The t -plane is cut along $[1, \infty)$ and paths of steepest descent either terminate at $t = 0$ (with $|\arg t| < \frac{1}{2}\pi$), $t = 1$ (with $|\arg(1 - t)| < \frac{1}{2}\pi$) or at infinity. Paths that approach infinity spiral round the point $t = 1$ passing onto adjacent Riemann surfaces. The figures reveal that there are two critical values of the phase θ , where the saddles t_0 and t_1 become connected (via a Stokes phenomenon). We denote these values by $\theta_0 \equiv \theta_0(\alpha)$ and $\theta_1 \equiv \theta_1(\alpha)$, where α is defined in (5.2). The values of these critical angles are tabulated in Table 3 for different α .

When $0 \leq \theta < \theta_0(\alpha)$, the integration path can be deformed to coincide with the steepest descent path passing over t_0 , so that the leading behaviour in (5.4) applies in this sector. When $\theta_0(\alpha) < \theta < \theta_1(\alpha)$, the integration path is deformed to pass over both saddles t_0 and t_1 , where each steepest descent path spirals out to infinity. Finally, when $\theta_1(\alpha) < \theta \leq \pi$, the integration path is deformed to pass over only the saddle t_1 .

Based on these considerations and on the approximation of the saddles $t_0 \simeq \alpha'^{\frac{1}{2}} - \frac{1}{2}\alpha'$, $t_1 \simeq 1 + \alpha' - \alpha'^3$, where $\alpha' = p/(4x)$, the leading behaviour of $B(x, y; p)$ is found to be

$$B(x, y; p) \sim \begin{cases} J_0 & 0 \leq \theta < \theta_1(\alpha) \\ J_0 - J_1 & \theta_1(\alpha) < \theta < \theta_2(\alpha) \\ J_1 & \theta_2(\alpha) < \theta \leq \pi \end{cases} \quad (5.6)$$

³The saddle t_2 does not enter into our consideration as it plays no role in the asymptotic evaluation of $B(x, y; p)$ when $0 \leq \theta \leq \pi$.

Table 3: Values of the critical angles θ_0 , θ_1 and θ^* as a function of $\alpha = p/(4|x|)$.

α	θ_0/π	θ_1/π	θ^*/π
0.30	0.603324	0.752315	0.688289
0.25	0.536784	0.798621	0.681218
0.20	0.476795	0.840611	0.672858
0.15	0.418651	0.879708	0.662628
0.10	0.358268	0.916935	0.649359
0.05	0.288029	0.953688	0.629820
0.01	0.198480	0.986248	0.597144

as $|x| \rightarrow \infty$ when $0 \leq \theta \leq \pi$ (with y and $p > 0$ finite), where

$$\begin{aligned} J_0 &:= \sqrt{\frac{2\pi}{|x|\psi''(t_0)}} t_0^{y-1} (1-t_0)^{x-1} \exp\left[\frac{-p}{4t_0(1-t_0)}\right] \\ &\sim \sqrt{\frac{\pi}{x}} \left(\frac{p}{4x}\right)^{\frac{1}{2}y-\frac{1}{4}} \exp\left[-(px)^{1/2} - \frac{3}{8}p\right] \end{aligned} \quad (5.7)$$

and

$$\begin{aligned} J_1 &:= \sqrt{\frac{2\pi}{|x|\psi''(t_1)}} t_1^{y-1} (1-t_1)^{x-1} \exp\left[\frac{-p}{4t_1(1-t_1)}\right] \\ &\sim i\sqrt{\frac{2\pi}{x}} \left(\frac{p}{4x}\right)^x e^{\pi ix} \exp\left[x - \frac{1}{4}p\right] \end{aligned} \quad (5.8)$$

with $\arg \psi''(t_r) \in [0, 2\pi]$, $r = 0, 1$. Inspection of Table 3 shows that as α decreases (that is, as $|x|$ increases for fixed p) the angular sector $\theta_0(\alpha) \leq \theta \leq \theta_1(\alpha)$, where $B(x, y; p)$ receives a contribution from both saddles, increases. We also show in Table 3 the value of $\theta = \theta^*(\alpha)$ at which $\Re(\psi(t_0)) = \Re(\psi(t_1))$ when the saddles are of the same height. We have $\theta_0(\alpha) < \theta^*(\alpha) < \theta_1(\alpha)$; then, for $\theta < \theta^*(\alpha)$ the saddle t_0 is dominant, whereas when $\theta > \theta^*(\alpha)$ the saddle t_1 is dominant in the large- $|x|$ limit.

In Table 4 we present the results of numerical calculations using the asymptotic behaviour of $B(x, y; p)$ in (5.6) compared to the values obtained by numerical integration of (5.1). The parameter values chosen correspond to $\alpha = 0.01$ and the saddles t_0 and t_1 are computed from (5.3), with the leading forms J_0 and J_1 computed from (5.7) and (5.8). It is seen from Table 3 that the exchange of dominance between the two contributory saddles arises for $\theta \simeq 0.60\pi$.

Appendix: A closed-form expression for the coefficients c_j

In this appendix we derive a closed-form expression for the coefficients c_j appearing in the expansion (2.2). Miller [4, Eq. (2.3a)] has shown that $B(x, y; p)$ can be expressed as a convergent series of Whittaker functions in the form

$$B(x, y; p) = 2^{1-x-y} \pi^{\frac{1}{2}} p^{(y-1)/2} e^{-\frac{1}{2}p} \sum_{k=0}^{\infty} \frac{(\frac{1}{2}y - \frac{1}{2}x)_k (\frac{1}{2} + \frac{1}{2}y - \frac{1}{2}x)_k}{k!} W_{-k-\frac{1}{2}y, \frac{1}{2}y}(p), \quad (A.1)$$

Table 4: Values of the asymptotic behaviour of $B(x, y; p)$ in (5.6) with the calculated value when $|x| = 50, p = 2$ ($\alpha = 0.01$) and $y = \frac{1}{2}$ for different $\theta = \arg x$.

θ/π	Asymptotic value	Calculated value
0	$+5.175 \times 10^{-06}$	$+5.187 \times 10^{-06}$
0.20	$-8.210 \times 10^{-06} + 2.081 \times 10^{-06}i$	$-8.223 \times 10^{-06} + 2.096 \times 10^{-06}i$
0.40	$+3.468 \times 10^{-05} - 6.934 \times 10^{-06}i$	$+3.470 \times 10^{-05} - 7.020 \times 10^{-06}i$
0.50	$+2.647 \times 10^{-06} - 9.853 \times 10^{-05}i$	$+2.402 \times 10^{-06} - 9.855 \times 10^{-05}i$
0.60	$-8.837 \times 10^{-04} - 3.821 \times 10^{-03}i$	$-8.781 \times 10^{-04} - 3.823 \times 10^{-03}i$
0.70	$-5.944 \times 10^{+28} + 1.659 \times 10^{+28}i$	$-5.952 \times 10^{+28} + 1.652 \times 10^{+28}i$
0.80	$+2.786 \times 10^{+54} + 3.451 \times 10^{+54}i$	$+2.786 \times 10^{+54} + 3.459 \times 10^{+54}i$
1.00	$+4.146 \times 10^{+77}$	$+4.154 \times 10^{+77}$

where $W_{\kappa, \mu}(x)$ is the Whittaker function. For $p \rightarrow \infty$ with bounded k , we have the expansion [7, Eq. (13.19.3)]

$$W_{-k-\frac{1}{2}y, \frac{1}{2}y}(p) = p^{-k-\frac{1}{2}} e^{-\frac{1}{2}p} \left\{ \sum_{n=0}^{N-1} (-1)^n \frac{(\frac{1}{2} + k)_n (y + \frac{1}{2} + k)_n}{n! p^n} + O(p^{-N}) \right\},$$

where N is a positive integer. Then we obtain from (A.1)

$$B(x, y; p) = 2^{1-x-y} \pi^{\frac{1}{2}} p^{-\frac{1}{2}} e^{-p} \{S(x, y; p) + O(p^{-N})\}, \tag{A.2}$$

where

$$\begin{aligned} S(x, y; p) &= \sum_{k=0}^{N-1} \frac{(\frac{1}{2}y - \frac{1}{2}x)_k (\frac{1}{2} + \frac{1}{2}y - \frac{1}{2}x)_k}{k! p^k} \sum_{n=0}^{N-1} (-1)^n \frac{(\frac{1}{2} + k)_n (y + \frac{1}{2} + k)_n}{n! p^n} \\ &= \sum_{k=0}^{N-1} \frac{(\frac{1}{2}y - \frac{1}{2}x)_k (\frac{1}{2} + \frac{1}{2}y - \frac{1}{2}x)_k}{k!} \sum_{j=k}^{N-1} (-1)^{j-k} \frac{(\frac{1}{2} + k)_{j-k} (y + \frac{1}{2} + k)_{j-k}}{(j-k)! p^j} + O(p^{-N}) \end{aligned}$$

and we have made the change of summation index $n \rightarrow j - k$. Use of the fact that $(-j)_k = (-1)^k j! / (j - k)!$, the above double sum can be written as

$$\begin{aligned} &\sum_{k=0}^{N-1} \frac{(\frac{1}{2}y - \frac{1}{2}x)_k (\frac{1}{2} + \frac{1}{2}y - \frac{1}{2}x)_k}{k!} \sum_{j=k}^{N-1} \frac{(-1)^j}{j!} \frac{\Gamma(j + \frac{1}{2}) \Gamma(y + j + \frac{1}{2})}{\Gamma(k + \frac{1}{2}) \Gamma(y + \frac{1}{2} + k) p^j} \\ &= \sum_{j=0}^{N-1} \frac{(-1)^j}{j!} \frac{(\frac{1}{2})_j (y + \frac{1}{2})_j}{j! p^j} \sum_{k=0}^j \frac{(-j)_k (\frac{1}{2}y - \frac{1}{2}x)_k (\frac{1}{2} + \frac{1}{2}y - \frac{1}{2}x)_k}{k! (\frac{1}{2})_k (y + \frac{1}{2})_k} \\ &= \sum_{j=0}^{N-1} \frac{(-1)^j}{j!} \frac{(\frac{1}{2})_j (y + \frac{1}{2})_j}{j! p^j} {}_3F_2 \left[\begin{matrix} -j, \frac{1}{2}y - \frac{1}{2}x, \frac{1}{2} + \frac{1}{2}y - \frac{1}{2}x \\ \frac{1}{2}, y + \frac{1}{2} \end{matrix} ; 1 \right]. \end{aligned} \tag{A.3}$$

upon reversal of the order of summation and identification of the inner sum over k as a terminating ${}_3F_2$ series of unit argument.

Comparison of (A.2) and (A.3) with the expansion obtained in (2.2) then yields the final result

$$c_j = \frac{(\frac{1}{2})_j (y + \frac{1}{2})_j}{j!} {}_3F_2 \left[\begin{matrix} -j, \frac{1}{2}y - \frac{1}{2}x, \frac{1}{2} + \frac{1}{2}y - \frac{1}{2}x \\ \frac{1}{2}, y + \frac{1}{2} \end{matrix} ; 1 \right]. \tag{A.4}$$

References

- [1] M. A. Chaudhry, A. Qadir, M. Rafique and S. M. Zubair, Extension of Euler's beta function, *J. Comp. Appl. Math.* **78** (1997) 19–32.
- [2] M. A. Chaudhry, A. Qadir, H. M. Srivastava and R. B. Paris, Extended hypergeometric and confluent hypergeometric functions, *Appl. Math. Comp.* **159** (2004) 589–602.
- [3] R. B. Dingle, *Asymptotic Expansions: Their Derivation and Interpretation*, Academic Press, London, 1973.
- [4] A. R. Miller, Remarks on a generalized beta function, *J. Comp. Appl. Math.* **100** (1998) 23–32.
- [5] J. L. López and P. J. Pagola, An explicit formula for the coefficients of the saddle point method, *Constr. Approx.* **33** (2011) 145–162.
- [6] G. Nemes, An explicit formula for the coefficients in Laplace's method by Lagrange interpolation, *Constr. Approx.* **38** (2013) 471–487.
- [7] F. W. J. Olver, D. W. Lozier, R. F. Boisvert and C. W. Clark (eds.), *NIST Handbook of Mathematical Functions*, Cambridge University Press, Cambridge, 2010.
- [8] R. B. Paris and D. Kaminski, *Asymptotics and Mellin-Barnes Integrals*, Cambridge University Press, Cambridge, 2001.
- [9] R. B. Paris, *Hadamard Expansions and Hyperasymptotic Evaluation: An Extension of the Method of Steepest Descents*, Cambridge University Press, Cambridge, 2011.
- [10] J. Wojdyło, On the coefficients that arise from Laplace's method, *J. Comp. Appl. Math.* **196** (2006) 241–266.

Received: March, 2015